

Supplemental material

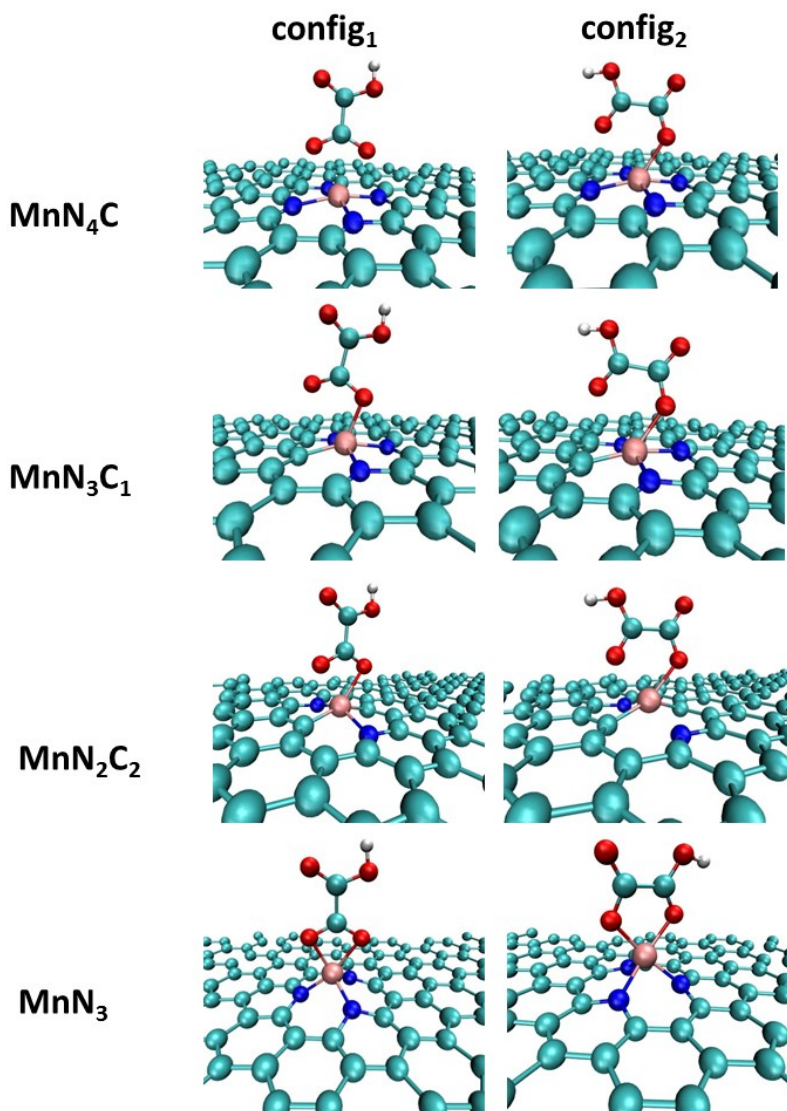


Figure S1. Most stable adsorption sites of $C_2O_4H^-$ anion on proposed active sites of Mn-AAPyr. Two possible adsorption configurations are shown.

Table S1. Change in the electronic energy, zero-point energy, and $T\Delta S$ term used to obtain the free energy diagram for oxalate oxidation mechanism on MnN_4 active sites of Mn-AAPyr at $pH=0$.

Reaction:	$\Delta E/eV$	$\Delta ZPE/eV$	$T\Delta S/eV$	$\Delta_r G/eV$
$*C_2O_4H + H^+ + e^- \rightarrow *C_2O_4H + H^+ + e^-$	+0.49	+0.09	-0.80	+1.38
$*C_2O_4H + H^+ + e^- \rightarrow CO_2H^* + CO_2 + H^+$	-0.31	-0.305	+0.66	-1.28
$CO_2H^* + CO_2 + H^+ + e^- \rightarrow 2CO_2 + 2H^+ +$	-0.03	-0.18	+0.86	-1.06

Table S2. Change in the electronic energy used to obtain the free energy diagram for oxalate oxidation mechanism on MnN₃C, MnN₂C₂, MnN₂C₂(2) and MnN₃ active sites of Mn-AAPyr at pH=0. Change in zero-point energy and $T\Delta S$ term are assumed to be the same for all active sites and are given in Table 1 .

Reaction:	$\Delta E/eV$			
	MnN ₃ C	MnN ₂ C ₂	MnN ₂ C ₂ (2)	MnN ₃
$*C_2O_4H + H^+ + e^- \rightarrow *C_2O_4H + H^+ + e^-$	0.03	-0.25	0.06	-1.79
$*C_2O_4H + H^+ + e^- \rightarrow CO_2H * + CO_2 + H^+$	0.18	0.39	0.13	1.13
$CO_2H * + CO_2 + H^+ + e^- \rightarrow 2CO_2 + 2H^+ + e^-$	-0.04	+0.02	-0.03	+0.82